

Low Cost Growth Route for Single-walled Carbon Nanotubes from Decomposition of Acetylene over Magnesia Supported Fe-Mo Catalyst

Md. Shahajan, Young Hwan Mo and Kee Suk Nahm[†]

School of Chemical Engineering and Technology, Chonbuk National University, Chonju 561-756, Republic of Korea

(Received 20 June 2002 • accepted 14 October 2002)

Abstract—A large amount of single wall carbon nanotubes (SWNTs) was successfully produced by thermal decomposition of C_2H_2 at 800 °C over magnesia supported Fe-Mo bimetallic catalysts in a tubular flow reactor under an atmosphere of hydrogen flow. The growth density of SWNTs increased with increasing the weight percent of the catalyst metals (wt% ratio of two metals: 50 : 50) supported on magnesia (MgO) from 5 to 30 wt%. The yield of SWNTs reached 144.3% over 30 wt% metal-loaded catalyst. Raman measurements showed the growth of bundle type SWNTs with diameters ranging from 0.81 to 1.96 nm. The growth of SWNTs was also identified by thermal gravimetric analysis (TGA) and Raman spectroscopy.

Key words: Single-Walled Carbon Nanotubes, Fe-Mo/MgO Catalyst, Low-Cost Growth, Acetylene, RTCVD

INTRODUCTION

Carbon nanotubes (CNTs) are attracting much attention because of their novel mechanical and electronic properties [Wong et al., 1997; Saito, 1997]. Since the electronic and mechanical properties of the single-walled nanotube (SWNT) can easily be theoretically studied compared with multi-walled nanotube (MWNT) [Mintmire et al., 1992], SWNTs have opened a great number of potential applications of the CNTs. However, the high cost of the current production methods and the difficulty in the large-scale manufacture of the CNTs have slowed down the process of bringing nanotube-based technologies to commercial practice.

SWNTs have been primarily synthesized by arc-discharge [Iijima and Ichihashi, 1993; Bethune et al., 1993] and laser ablation [Guo et al., 1995] techniques. The two methods may not be good for achieving a continuous process of SWNT production for a commercial purpose because of their low CNT yield and difficulty of eliminating the growth of unwanted carbon products like soot. A recently reported synthesis method of SWNTs using catalytic decomposition of carbon-containing molecules on pre-formed catalytic particles is proposed to be a unique development to large-scale production [Peigney et al., 1997; Colomer et al., 2000; Kitiyanan et al., 2000]. The main advantage of the catalytic growth method lies in the simplicity of the process under mild conditions and in the higher yield of carbon nanotubes. Moreover, the size and the density of CNTs are controllable by uniformly dispersing catalyst particles on supports and/or by adjusting reaction parameters [Peigney et al., 1997; Colomer et al., 2000; Kitiyanan et al., 2000; Kibria et al., 2001]. It was observed that a mixture of single- and multi-walled nanotubes was produced from decomposition of CH_4 at 1,050 °C over alumina-supported Fe catalyst without quantifying each component in the mixture [Peigney et al., 1997]. The growth of SWNTs including small amount of double-wall nanotubes was also reported

by disproportionation of CO over alumina-supported Mo particles at 1,200 °C [Dai et al., 1996]. The key factor for the catalytic growth of SWNT is to maintain a certain critical size of small metal catalyst particles. The size was achieved by using lower metal loading content (around 10 wt%) in supported catalysts [Peigney et al., 1997; Colomer et al., 2000; Kitiyanan et al., 2000; Dai et al., 1996]. As a result the yield of the nanotubes remains low. Longer catalytic activity was observed from highly loaded bimetallic supported catalyst for the growth of CNTs [Kibria et al., 2001]. Alvarez et al. [2001] recently found that molybdenum component in the catalyst stabilizes small cobalt particles in the course of the growth reaction, which are highly selective to the production of SWNT. Tang et al. [2001] showed that total carbon yield was 215% with >80 wt% SWNT in growth of CNTs by the decomposition of H_2/CH_4 over $Mo_{0.05}Co_{0.05}Mg_{0.9}O$ catalyst at 1,000 °C.

The present study aims to synthesize SWNTs over MgO supported Fe-Mo bimetallic catalysts by using C_2H_2/H_2 flowing gas mixtures under controlled conditions, and attempts to exploit the potential role of molybdenum in the catalysts. To optimize the production condition of SWNTs, we have studied the growth of carbon nanotubes varying the metal loading in the catalysts and using molybdenum as a moderator for stabilizing small catalyst particles active to grow SWNTs. The structural properties of the grown SWNTs were identified by various analytic techniques.

EXPERIMENT

We prepared one set of magnesia (MgO) supported bimetallic (Fe-Mo) catalysts using impregnation. The weight percents of the two metals in the catalysts were 5, 10, 20, 30 and 40. A calculated amount of $[Fe(NO_3)_3 \cdot 9H_2O]$ and $[(NH_4)_6Mo_2O_24 \cdot 4H_2O]$ was dissolved in DI water with 1 : 1 weight ratio of the two metals. The prepared aqueous solution was mixed with required amount of MgO powders and was stirred at around 70 °C to remove dissolved oxygen and attain a homogeneous impregnation of the metal salts on the MgO support until water thoroughly evaporated. The impreg-

[†]To whom correspondence should be addressed.

E-mail: nahmks@moak.chonbuk.ac.kr

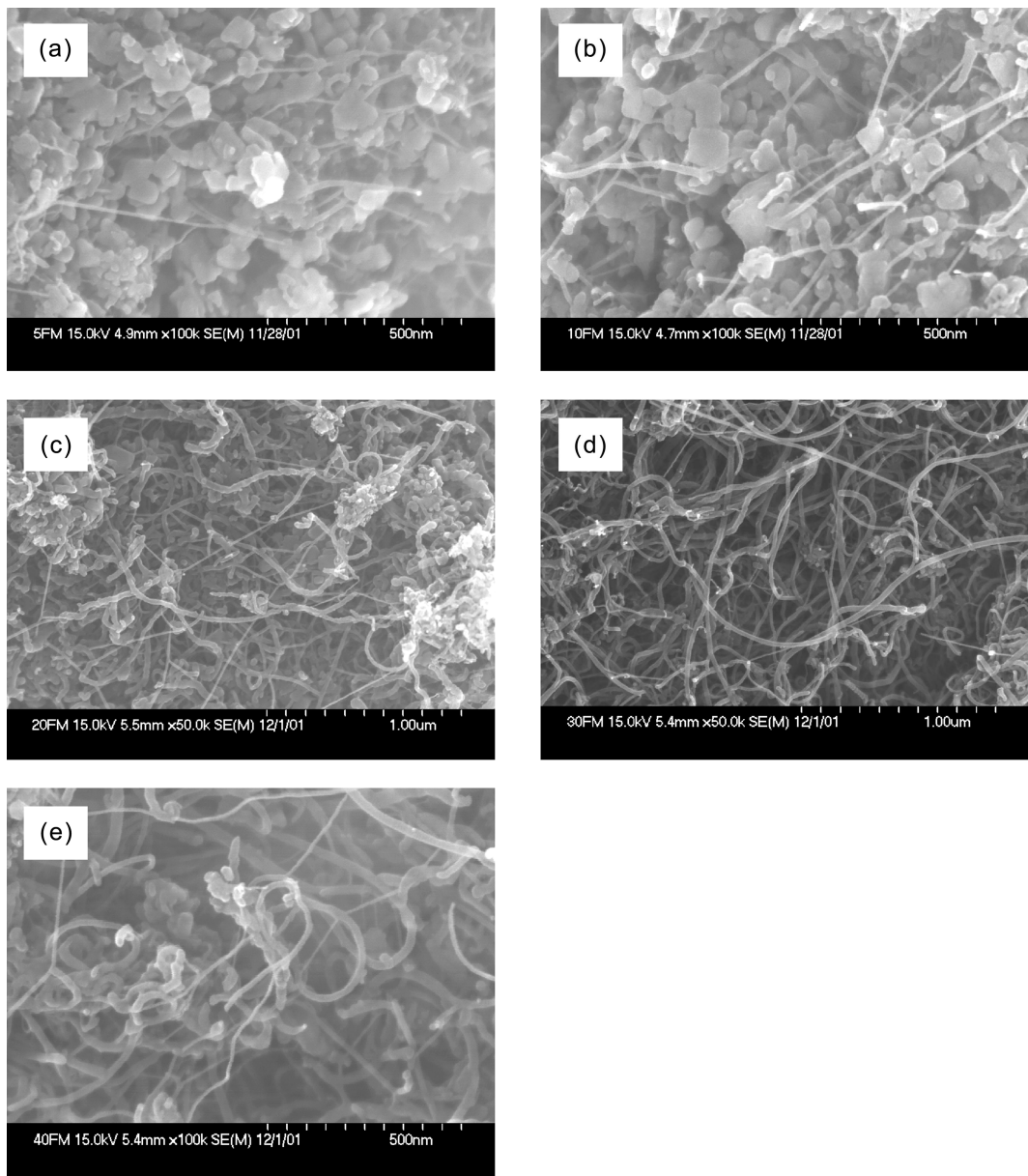


Fig. 1. SEM images of CNTs grown over Fe-Mo/MgO catalysts for 30 min at 800 °C with $C_2H_2/H_2=10/100$ sccm (a) 5%, (b) 10%, (c) 20%, (d) 30% and (e) 40% metals (Fe, Mo), respectively.

ate was then further dried in an oven at 100 °C for 12 hrs and the dried product was calcined at 400 °C for 6 hrs in a box furnace to form a powder product. The powders were reduced at 450 °C for 4 hrs in 100 sccm (standard cubic centimeter per minute) hydrogen flow under a vacuum (10 torr). The produced supported catalysts were stored in sealed vessels and were used for the growth of CNTs.

Approximately 20 mg of a catalyst was uniformly dispersed in the base area of a quartz plate and placed in the central hot region of a horizontal quartz tube reactor. The catalyst was activated at 500 °C for 1 h in the reactor under H_2 flows (100 sccm) and then the growth of CNTs was carried out at 800 °C by flowing C_2H_2/H_2 (10/100 sccm). Carbon yields were measured after growing CNTs for 30 min over catalysts. The structure and morphology of the synthesized CNTs were characterized by using scanning electron microscopy (SEM), thermal gravimetric analysis (TGA), and FT-Raman spectroscopy.

RESULTS AND DISCUSSION

Fig. 1 presents the SEM images for CNTs grown over MgO-supported Fe-Mo catalysts, as a function of metal catalyst content. The CNTs were grown for 30 min at 800 °C with C_2H_2/H_2 (10/100 sccm) over the catalysts whose metal loading weight percent varies from 5 to 40 wt%. The growth density of the CNTs increases with the metal loading weight percent. Over 20 wt%, the catalyst surface is completely covered with CNTs, and a close observation of the SEM images shows that every metal particle seeded the growth of carbon nanotubes with a regulated diameter. However, 5 and 10 wt% metal loaded catalysts grow small amount of CNTs, but they mostly form amorphous carbon.

The average outer diameter of the grown CNTs is approximately 10-20 nm and the average tube length seems to reach several mi-

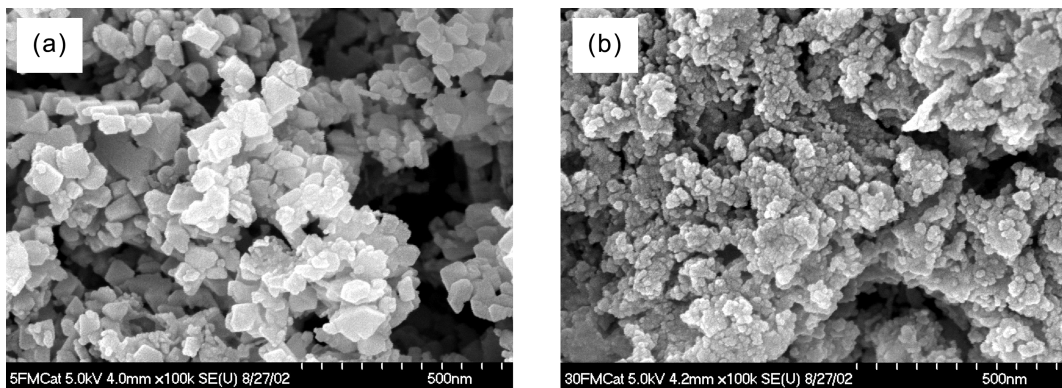


Fig. 2. SEM images of Fe-Mo/MgO catalysts with metals loading (a) 5 and (b) 30 wt%, respectively.

cron scales. But it was hard to measure the accurate length of individual filament because both the ends of the tubes are unclearly observed from the pictures. The diameter of individual CNT seems to thicken with an increase of the metal loading content over the catalysts.

Fig. 2 (a and b) represent the SEM images of catalysts with metals loading 5 and 30 wt%, respectively. It is clearly observed from these SEM figures that the catalyst particle size dramatically decreased with the increase metals loading in the catalysts. Comparing Fig. 2 (a and b) with Fig. 1 (a and d), we can conclude that catalysts with higher metals loading are very active to grow CNTs due to the smaller catalyst particle size.

We also investigated the activity of our prepared catalysts for the growth of CNTs. Fig. 3 presents the carbon yields for the catalysts as a function of the metal loading content in the catalysts. Carbon yield (deposited carbon during reaction) was calculated by using the following equation:

$$\text{Carbon yield (\%)} = [(m_{\text{tot}} - m_{\text{cat}})/m_{\text{cat}}] \times 100$$

where m_{cat} and m_{tot} are the catalyst weights before and after the growth reaction, respectively. Therefore, m_{cat} is the initial weight of the catalyst loaded for the reaction, while m_{tot} is the total weight (catalyst + carbon) measured after the reaction. Carbon yield (%) linearly increases up to 30 wt% metal loading and then decreases from 30 to 40 wt% in this work.

It seems that the growth density and yield of CNTs strongly depend on carbon source feeding rate and metal loading content. Since the CNTs were grown at 800 °C at a fixed flow rate of acetylene in the experiment, it is thought that the growth density and yield naturally increases with increasing the metal loading content in the catalysts. Literature [Hafner et al., 1998] reported that the amount of carbon source supplied to catalyst surface is the key factor for the formation of the nanotubes. They observed the formation of MWNT or amorphous carbon at higher carbon supply rates. But they were able to grow SWNTs at a limited supply rate of carbon source. In our experiments, it is likely that the formation of amorphous carbon is observed over 5 and 10 wt% of metal loadings instead of the formation of CNTs since acetylene inclines to catalytically decompose at lower temperature [Kibria et al., 2001; Hemadi et al., 1996]. Amorphous carbon seems to readily form at sufficient carbon source and lower catalyst content. We speculate that the agglomeration of some Fe-Mo catalyst particles might diminish the growth density

and yield of the CNTs. It is thought that the increase of the metal loading in the Fe-Mo/MgO catalyst escalates the agglomeration of the catalyst particles, resulting in the decrease of the CNT growth at higher metal loading contents, as was seen by comparing the yields over 30 and 40 wt% Fe-Mo/MgO catalysts.

To clarify the effect of a specific metal in the catalysts on the CNT's growth, we prepared two monometallic catalysts whose compositions are 30 wt% Fe/MgO (iron catalyst), and 30 wt% Mo/MgO (molybdenum catalyst). We investigated the carbon yield as well as the morphology of CNTs grown over the monometallic catalysts at the same experimental condition. Deposited carbon yields (%) were 4.93 and 49.6 for MgO supported monometallic molybdenum and iron catalysts, respectively. The carbon yields obtained from the monometallic catalysts were remarkably lower than those observed for the bimetallic catalysts in Fig. 3. After carbon deposition over the monometallic catalysts, SEM images (Fig. 4) reveal that the molybdenum catalyst is inactive to the growth of CNTs in the experimental range we investigated here. These observations confirmed that molybdenum was inactive to grow CNTs in our experimental conditions (although 4.93% carbon deposited), but the addition of iron to molybdenum dramatically increased catalytic activity to grow large amount of CNTs. We speculate that molyb-

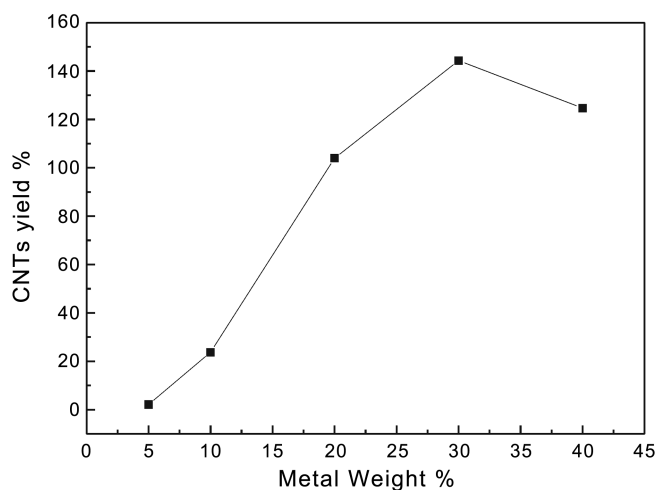


Fig. 3. Variation of deposited carbon yield with metal wt% in the catalysts, CNTs grown for 30 min at 800 °C with $\text{C}_2\text{H}_2/\text{H}_2 = 10/100$ sccm.

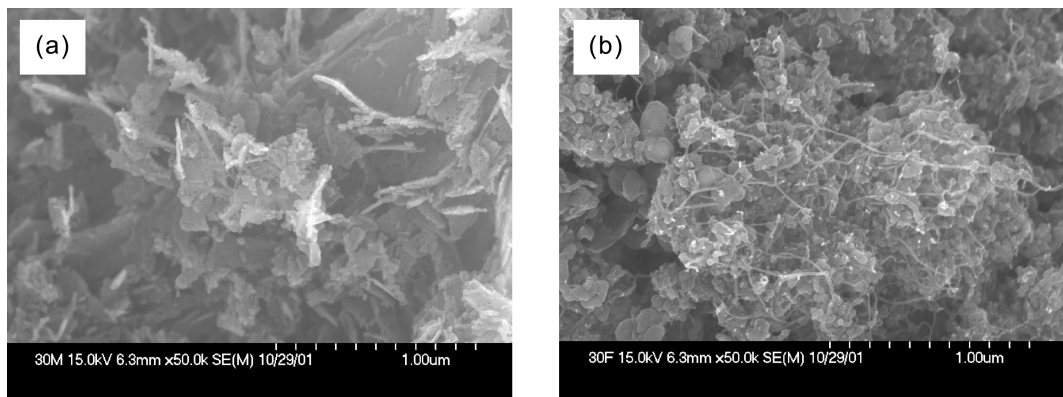


Fig. 4. SEM images of CNTs grown for 30 min at 800 °C with $C_2H_2/H_2=10/100$ sccm (a) 30 wt% Mo/MgO catalyst and (b) 30 wt% Fe/MgO catalyst, respectively.

denum undergoes a phase transformation from oxide to carbide [Alvarez et al., 2001] and contributes to the stabilization of the active metal (Fe) particles for the CNTs growth. This facilitates that the bimetallic catalysts became more active even at higher metal loading contents. Alvarez et al. [2001] measured X-ray absorption near-edge spectra (XANES) for silica-supported Co-Mo catalyst employed for the growth of SWNTs. They found that oxide species such as MoO_3 , Co_3O_4 and $CoMoO_4$ coexist in thermally treated catalyst before the CNTs' growth, but the catalysts contain only metallic cobalt, Mo-carbide, and small amount of Mo-oxide after the CNTs growth for 30 min. They proposed that the role of Mo is a moderator to increase the activity of Co catalyst for the CNTs growth. They concluded that the role of molybdenum in the catalyst is to stabilize small particles of oxidized cobalt species, which are highly selective to the production of SWNT.

Fig. 5 shows TGA curve for CNTs grown over 20 wt% Fe-Mo/MgO catalyst. The TGA was measured under the flow of 100 sccm $Ar : O_2$ (92 : 8 v/v) mixed gas, varying temperature from room temperature to 1,000 °C with a heating rate of 5 °C/min. The weight loss is due to the combustion of carbons in the grown samples by O_2 . The residual weight at high temperatures is due to metal oxides

produced from the catalyst. The weight loss is very small below 400 °C and one step large weight loss commences at around 400 °C and ends at around 600 °C (Fig. 5). Thermal analysis of carbon nanotubes has been investigated by a few researchers. Kitiyanan et al. [2000] and Tang et al. [2001] reported that the oxidative temperatures were around 330 °C for amorphous carbon, 500-600 °C for SWNT, and 700 °C for MWNT, respectively. Shi et al. [2000] and Park et al. [2002] quantified the fractions of different carbonaceous products among arc grown SWNTs by differential thermogravimetric (DTG) analysis. The TGA curve of our grown CNTs over the catalysts is very similar to those of SWNTs observed in the above literature. The inset on the right top of Fig. 5 shows differential thermal analysis (DTA) curves for the grown CNTs. The DTA curve shows three stepwise burning temperatures at ~200, 500, and 930 °C, respectively, for the sample. This means that our grown nanotubes are composed of amorphous carbon, SWNTs, and MWNTs with graphite nanoparticle [Shi et al., 2000; Park et al., 2002]. But the TGA curve showed that more than 90% weight losses were observed at the temperature range of 400-600 °C, while the rest of the weight loss occurs at low temperatures below 400 °C and at high temperatures above 600 °C. Based on the TGA and DTA analyses, it is concluded that our grown CNTs are primarily SWNTs.

Raman spectroscopy is widely used for the characterization of CNT structures by measuring optical phonon frequencies [Cowley et al., 1997]. To confirm the presence of SWNT in our grown samples, Raman measurements were conducted at room temperature by using an excitation wavelength of 1,064 nm (Nd : YAG laser) for the CNT grown at 800 °C under 10/100 sccm C_2H_2/H_2 flow for 30 min over 30 wt% metal loaded Fe-Mo/MgO catalyst and the measured spectra was presented in figure. The Raman spectra exhibit three main zones at low ($100-300\text{ cm}^{-1}$), intermediate ($300-1,350\text{ cm}^{-1}$) and high ($1,500-2,000\text{ cm}^{-1}$) frequencies, respectively. The Raman scattering peak positions at low frequency region ($\omega \leq 500\text{ cm}^{-1}$) for SWNTs are strongly tube diameter dependence [Rao et al., 1997]. [The inset on the left top of Fig. 6 reveals that the low frequency band group consists of several small peaks appearing at 114, 145, 152, 167, 182, 208, 222, 230, 261 and 277 cm^{-1} , respectively, for our sample (spectrum a)].

Rao et al.'s [1997] theoretical study suggested that the peaks observed at the frequency range of $114-208\text{ cm}^{-1}$ correspond to A_{1g} and E_{1g} symmetries of the armchair (n, n) type tubes with $n=8$ to

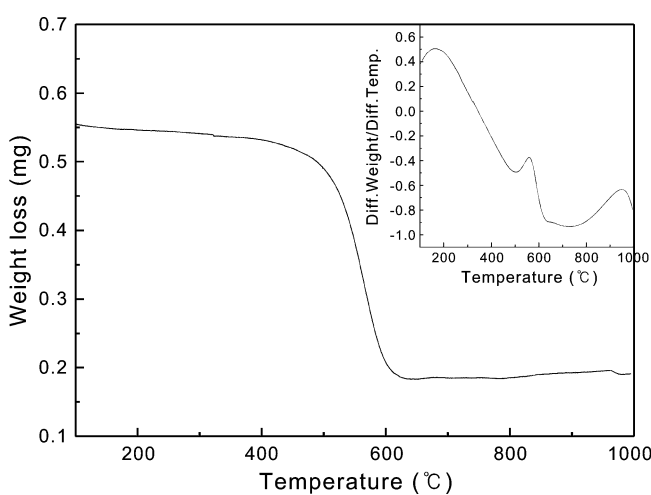


Fig. 5. TGA curves for CNTs grown over 20 wt% Fe-Mo/MgO catalyst for 30 min at 800 °C with $C_2H_2/H_2=10/100$ sccm. The inset shows the DTA curve for the same sample.

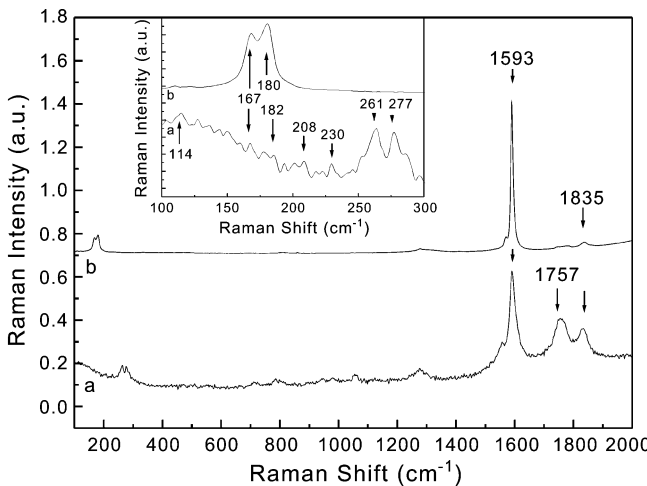


Fig. 6. FT-Raman spectra for CNTs grown over (a) 30 wt% Fe-Mo/MgO catalyst for 30 min at 800 °C with $\text{C}_2\text{H}_2/\text{H}_2=10/100$ sccm and (b) SWNTs purchased from Smalley's group. The inset shows details of the peak distribution in the low frequency range.

11 and determined that they are the radial breathing mode (RBM) for SWNTs. It was confirmed that the peaks at 167 and 230 cm^{-1} are due to the existence of (17, 0) and (13, 0) zigzag tubes, respectively [Kuzmany et al., 1998]. Theoretical arguments [Bandow et al., 1998], which were raised from force constant model calculations for the RBM frequency of SWNT with diameter less than 1.65 nm, proposing that 15 different radial mode frequencies might emerge between chiral integers (5, 5) and (12, 12) and seven of the anticipated frequencies must be chiral (n, m) symmetry tubes. Comparing the results of the theoretical and experimental studies [Rao et al., 1997; Bandow et al., 1998], it is thought that the Raman peaks at 261 cm^{-1} and 277 cm^{-1} are due to SWNTs with (7, 7) and (6, 6) symmetries, respectively. Symmetry of the peak at 222 cm^{-1} is still unclear, but a peak was observed at 221 cm^{-1} from the SWNTs grown by laser evaporation method [Kuzmany et al., 1998].

The relationship between the tube diameter and the Raman frequency of the breathing mode can be estimated by using the formula $\omega=223.75/d$ [Bandow et al., 1998], where d is the diameter of the tube in nanometers and ω is the frequency of the radial breathing mode in cm^{-1} . The calculation showed that the RBM frequencies of 114, 145, 152, 167, 182, 208, 222, 230, 261 and 277 cm^{-1} correspond to the tube diameters of 1.96, 1.54, 1.47, 1.34, 1.23, 1.08, 1.01, 0.97, 0.86 and 0.81 nm, respectively.

Summarizing the above discussion based on the literature survey, the RBM frequencies observed in this work strongly support the growth of SWNTs with diameters ranging from 0.81 to 1.96 nm. Consequently, Raman analysis proposes the tubes observed in SEM are composed of bundle type SWNTs. The SWNT bundles form due to a van der Waals force. It is likely that the SWNT bundles mechanically twist or knit together to form long and wide ropes or ribbons, and then thin layers of amorphous carbon cover the SWNT bundles, which exhibit very uniform tubes with individual diameters. According to the theoretical predictions, the frequency of the RBM is inversely proportional to the tube diameter without any chirality dependence. The calculation of formation energies using a

force constant model [Rao et al., 1997; Bandow et al., 1998] proposes that (n, n) armchair tubes with n=6 to 11 are the most stable SWNT species in our observed diameter range. From lower frequency range [inset (spectrum a) of Fig. 6], it can also be seen that the Raman peak corresponding to (6, 6) and (7, 7) at the frequency range 277 and 261 cm^{-1} , respectively, is stronger than others, indicating that the (6, 6) and (7, 7) nanotube in the sample might be more abundant than the others. To clarify the spectrum of our grown nanotubes, we measured the Raman spectrum of purchased SWNTs (Smalley group, Rice University USA) and compared the result with the Raman spectrum of our sample. The Raman spectra are almost similar patterns with those of our samples as shown in spectrum (b) of Fig. 6. The dissimilarities of the Raman spectra are in the RBM peak position (two RBM peaks observed at 167 and 180 cm^{-1}). For our sample the RBM peak arose at a higher wave number indicating that our sample contains SWNTs with thinner diameter.

The high frequency group of bands consists of three resolved peaks at 1,593, 1,757 and 1,835 cm^{-1} , respectively. The peak at 1,757 cm^{-1} results from the second-order Raman process involving the combination of the RBM and the tangential mode (G-line) at 1,593 cm^{-1} , which strongly supports the growth of SWNTs. The peak at 1,593 cm^{-1} seems to appear due to the C-C stretching Raman active Eg modes, indicating the formation of graphitic sheets. The unresolved shoulder triplet peaks (A_{1g} , E_{1g} , E_{2g}) at 1,535, 1,550 and 1,562 cm^{-1} have been confirmed to be due to the growth of SWNTs from theoretical calculations [Rao et al., 1997]. The peak at 1,827 cm^{-1} is unclear, but the peak was observed at 1,825 cm^{-1} from SWNTs grown by arc-discharge method reported in previous work [Mo et al., 2001].

Several weak features are also observable significantly in the frequency range of 300-1,350 cm^{-1} . Most of them were identified to be due to overtones and combinations of lower frequency modes [Chapelle et al., 1998]. The intensity of the weak overtones peaks located below 600 cm^{-1} is approximately twice that of lower frequency bands. The peak at 1,273 cm^{-1} (D_1 band) indicates the formation of the polycrystalline graphitic carbon materials, but the appearance of no peak at around 1,327 cm^{-1} (D_2 band) ensures the absence of MWNTs or disordered amorphous carbon [Chapelle et al., 1998]. The presence of a mode at 797 cm^{-1} clearly shows the existence of armchair tubes with n, ranging from 6 to 12, as was theoretically proposed elsewhere [Eklund et al., 1995]. The peak near 718 cm^{-1} has specified the growth of zigzag tubes [Chapelle et al., 1998]. In Raman spectra, D band shape is very sensitive to the structural disorder present in carbons. For polycrystalline samples, the D band emerging at 1,285 cm^{-1} (D_1) is attributed to disordered or sp^3 -hybridized carbons in the hexagonal framework of the nanotube walls, while it appears as a broad feature centered between 1,311 cm^{-1} and 1,327 cm^{-1} (D_2) for the amorphous carbon spectra. In comparison with the Raman spectra reported for SWNTs and MWNTs, the presently observed result obviously reveals the growth of SWNTs. In this work, it was seen that the tangential mode at 1,593 cm^{-1} (G-line) has three shoulder peaks at 1,535, 1,550 and 1,562 cm^{-1} and a peak for RBM mode peaks appear at around 277 cm^{-1} . Moreover, the high intensity ratio of tangential mode (G-line) to the D band indicates the formation of the ordered crystalline of carbonaceous product.

CONCLUSIONS

In conclusion, a large amount of SWNTs could be produced successfully by rapid thermal chemical vapor deposition (RTCVD) method from catalytic decomposition of C_2H_2 at 800 °C in H_2 atmosphere. We have established how to control the growth density of SWNTs by varying the metal loading in the catalyst and observed 20 to 30 wt% metals loaded Fe-Mo binary system with 1 : 1 wt ratio of the two metals produced high performance selective catalysts to grow large amount of SWNTs. High-density SWNTs with diameter ranging from 0.81 to 1.96 nm were bundle type that was measured by Raman spectra and tubes composed of homogeneous bundles of diameter around 10 to 20 nm. Molybdenum, inactive to CNTs growth in the experimental conditions investigated, largely increases the yield of SWNTs when added with Fe in supported bimetallic catalysts. 144.3 yield % of good quality SWNTs was achieved over 30 wt% metals loaded Fe-Mo/MgO catalyst. TGA analysis was performed to identify the different types of carbon species, and the one step TGA graph shows more than 90% weight loss in between 400-600 °C and indicates that our grown nanotube is dominated by SWNTs. Raman spectra were exclusively used to characterize the growth of SWNTs as well as diameter distribution, and the degree of crystalline perfection was also investigated.

ACKNOWLEDGMENTS

This work was supported by KOSEF through the Research Center for Energy Conversion and Storage

REFERENCES

- Alvarez, E. W., Kitiyanan, B., Borgna, A. and Resasco, E. D., "Synergism of Co and Mo in the Catalytic Production of Single-wall Carbon Nanotubes by Decomposition of CO," *Carbon*, **39**, 547 (2001).
- Bandow, S., Asaka, S., Saito, Y., Rao, A. M., Grigorian, L., Richter, E. and Eklund, P. C., "Effect of the Growth Temperature on the Diameter Distribution and Chirality of Single-Wall Carbon Nanotubes," *Phys. Rev. Lett.*, **80**, 3779 (1998).
- Bethune, S. D., Kiang, H. C., de Vries, S. M., Gorman, G., Savoy, R., Vazquez, J. and Beyers, R., "Cobalt-Catalysed Growth of Carbon Nanotubes with Single-atomic-layer Walls," *Nature*, **363**, 605 (1993).
- Chapelle De La Lamy, M., Lefrant, S., Journet, C., Maser, W., Bernier, P. and Loiseau, A., "Raman Studies on Single Walled Carbon Nanotubes Produced by the Electric Arc Technique," *Carbon*, **36**(5-6), 705 (1998).
- Colomer, J.-F., Stephan, C., Lefrant, S., Tendeloo, V. G., Willems, I., Konya, Z., Fonseca, A., Laurent, Ch. and Nagy, B. J., "Large-scale Synthesis of Single-wall Carbon Nanotubes by Catalytic Chemical Vapor Deposition (CCVD) Method," *Chem. Phys. Lett.*, **317**, 83 (2000).
- Cowley, Y. J. M., Nikollaev P., Thess, A. and Smalley, E. R., "Electron Nano-diffraction Study of Carbon Single-walled Nanotube Ropes," *Chem. Phys. Lett.*, **265**, 379 (1997).
- Dai, H., Rinzel, G. A., Nikollaev, P., Thess, A., Colbert, T. D. and Smalley, E. R., "Single-wall Nanotubes Produced by Metal-catalyzed Disproportionation of Carbon Monoxide," *Chem. Phys. Lett.*, **260**, 471 (1996).
- Eklund, P. C., Holden, J. M. and Jishi, R. A., "Vibrational Modes of Carbon Nanotubes; Spectroscopy and Theory," *Carbon*, **33**(7), 959 (1995).
- Guo, T., Nikollaev, P., Thess, A., Colbert, T. D. and Smalley, E. R., "Catalytic Growth of Single-walled Nanotubes by Laser Vaporization," *Chem. Phys. Lett.*, **243**, 49 (1995).
- Hafner, H. J., Bronikowski, J. M., Azamian, R. B., Nikollaev, P., Rinzel, G. A., Colbert, T. D., Smith, A. K. and Smalley, E. R., "Catalytic Growth of Single-wall Carbon Nanotubes from Metal Particles," *Chem. Phys. Lett.*, **269**, 195 (1998).
- Hernadi, K., Fonseca, A., Nagy, B. J., Bernaerts, D. and Lucas, A. A., "Fe-Catalyzed Carbon Nanotube Formation," *Carbon*, **34**(10), 1249 (1996).
- Iijima, S. and Ichihashi, T., "Single-shell Carbon Nanotubes of 1-nm Diameter," *Nature*, **363**, 603 (1993).
- Kibria Fazle, A. K. M., Mo, Y. H. and Nahm, K. S., "Synthesis of Carbon Nanotubes over Nickel-iron Catalysts Supported on Alumina Under Controlled Conditions," *Cat. Lett.*, **71**(3-4), 229 (2001).
- Kibria Fazle, A. K. M., Mo, Y. H., Yun, M. H., Kim, J. M. and Nahm, K. S., "Effect of Bimetallic Catalyst Composition and Growth Parameters on the Growth Density and Diameter of Carbon Nanotubes," *Korean J. Chem. Eng.*, **18**(2), 208 (2001).
- Kitiyanan, B., Alvarez, E. W., Harwell, H. J. and Resasco, E. D., "Controlled Production of Single-wall Carbon Nanotubes by Catalytic Decomposition of CO on Bimetallic Co-Mo Catalysts," *Chem. Phys. Lett.*, **317**, 497 (2000).
- Kuzmany, H., Burger, B., Thess, A. and Smalley, R. E., "Vibrational Spectra of Single Wall Carbon Nanotubes," *Carbon*, **36**(5-6), 709 (1998).
- Mintmire, W. J., Dunlap, I. B. and White, T. C., "Are Fullerene Tubules Metallic," *Physical Rev. Lett.*, **68**(5), 631 (1992).
- Mo, Y. H., Kibria, A. K. M. F. and Nahm, K. S., "The Growth Mechanism of Carbon Nanotubes from Thermal Cracking of Acetylene over Nickel Catalyst Supported on Alumina," *Synthetic Metals*, **122**, 443 (2001).
- Park, Y. S., Kim, K. S., Jeong, H. J., Kim, W. S., Moon, J. M., An, K. H., Bae, D. J., Lee, Y. S., Park, G.-S. and Lee, Y. H., "Low Pressure Synthesis of Single-walled Carbon Nanotubes by Arc Discharge," *Synthetic Metals*, **126**, 245 (2002).
- Peigney, A., Laurent, Ch., Dobigeon, F. and Rousset, A., "Carbon Nanotubes Grown *in situ* by a Novel Catalytic Method," *J. Mater. Res.*, **12**(3), 613 (1997).
- Rao, A. M., Richter, E., Bandow, S., Chase, B., Eklund, P. C., Williams, K. A., Fang, S., Subbaswamy, K. R., Menon, M., Thess, A., Smalley, R. E., Dresselhaus, G. and Dresselhaus, M. S., "Diameter-Selective Raman Scattering from Vibrational Modes in Carbon Nanotubes," *Science*, **275**, 187 (1997).
- Saito, S., "Carbon Nanotubes for Next-Generation Electronics Devices," *Science*, **278**, 77 (1997).
- Shi, Z., Lian, Y., Liao, F. H., Zhou, X., Gu, Z., Zhang, Y., Iijima, S., Li, H., Yue, T. K. and Zhang, S.-L., "Large Scale Synthesis of Single-wall Carbon Nanotubes by Arc-discharge Method," *J. Physics and Chemistry of Solids*, **61**, 1031 (2000).
- Tang, S., Zhong, X. Z., Sun, L., Liu, L., Lin, J., Shen, X. Z. and Tan, L. K., "Controlled Growth of Single-walled Carbon Nanotubes by Catalytic Decomposition of CH_4 over Mo/Co/MgO Catalysts," *Chem. Phys. Lett.*, **350**, 19 (2001).
- Wong, W. E., Sheehan, E. P. and Lieber, M. C., "Nanobeam Mechanics: Elasticity, Strength, and Toughness of Nanorods and Nanotubes," *Science*, **277**, 1971 (1997).